DOI: 10.1002/cssc.201300438

Design, Synthesis, and Evaluation of Nonaqueous Silylamines for Efficient CO_2 Capture

Jackson R. Switzer,[a] Amy L. Ethier,[a] Emily C. Hart,[b] Kyle M. Flack,[b] Amber C. Rumple,[b] Jordan C. Donaldson,[a] Ashley T. Bembry,[a] Owen M. Scott,[a] Elizabeth J. Biddinger,[a] Manish Talreja,[a] Myoung-Geun Song,[b] Pamela Pollet,[b] Charles A. Eckert,[a, b] and Charles L. Liotta*[a, b]

A series of silylated amines have been synthesized for use as reversible ionic liquids in the application of post-combustion carbon capture. We describe a molecular design process aimed at influencing industrially relevant carbon capture properties, such as viscosity, temperature of reversal, and enthalpy of regeneration, while maximizing the overall CO_2-capture capacity. A strong structure–property relationship among the silylamines is demonstrated in which minor structural modifications lead to significant changes in the bulk properties of the reversible ionic liquid formed from reaction with CO_2.

Introduction

Despite efforts to develop alternative, carbon-neutral energy sources, it is projected that coal will remain the predominant fuel for electricity generation until 2035.[1,2] Coal-fired power plants produce nearly a third of all CO_2 emissions in the United States, which represent large point sources of CO_2 emissions.[3] With the growing recognition that global CO_2 emissions must be reduced to mitigate their harmful environmental impact, there is significant interest in the development of post-combustion CO_2-capture technologies that can be retrofitted to existing power plants.[4]

Several gas separation technologies applicable to CO_2 capture are in use today; their feasibility and cost-effectiveness are highly dependent on capture conditions (e.g., temperature, pressure, concentration) and purity specifications at release.[4,5] One of the most mature technologies is the use of an absorption-based process. In general, viable absorption-based, post-combustion CO_2-capture processes must meet three criteria. First, the liquid sorbent must be selective for CO_2, which comprises only a portion of post-combustion coal-fired power plant flue gas (approximately 16% by volume).[6,7] Second, the system must also be recyclable; the amount of CO_2 released by just one coal-fired power plant in a year of operation makes capture by a single-use sorbent unfeasible.[6] Finally, the system must operate in a cost-effective manner and minimize the overall energy required for capture and release.[2]

Reversible ionic liquids have been developed as a new class of switchable solvents.[8] Our recent work has focused on reversible ionic liquids derived from silylamines.

An example of the basic silylamine structure and its reaction with CO_2 is shown in Scheme 1. Upon reaction with CO_2, silylamines reversibly form an ammonium carbamate salt, which is liquid at or near room temperature; the salt is referred to as the reversible ionic liquid. On heating, the reversible ionic liquid releases the captured CO_2 to reform the silylamine. We previously demonstrated the use of this type of solvent system in coupling reactions and separations[9] as well as in crude oil separation.[10] Most recently, we have shown how reversible ionic liquids can be used as a unique class of CO_2-absorption solvents.[11] In addition, we have shown that the reversible ionic liquid is further capable of physically absorbing additional CO_2.[11] This dual method of capture provides enhanced CO_2 uptake under industrially relevant operating conditions.[12]

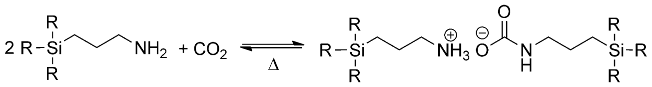

Scheme 1. Example trialkylsilamine and its reaction equilibrium with CO_2.

Here we describe how we have used iterative molecular design to optimize the structures of silylamines for CO_2 capture and show how the variation of the length of the tether that connects the amine to the Si atom and changing the position of or the addition of a single methyl group to the silylamine backbone can influence capture properties.

We present 13 silylated amines (Table 1) as potential candidates for an absorption-based CO_2-capture process and show

---

[a] J. R. Switzer, A. L. Ethier, J. C. Donaldson, A. T. Bembry, O. M. Scott, E. J. Biddinger, M. Talreja, Prof. C. A. Eckert, Prof. C. L. Liotta
School of Chemical and Biomolecular Engineering
Georgia Institute of Technology
311 Ferst Street, Atlanta, GA 30332 (USA)

[b] E. C. Hart, K. M. Flack, A. C. Rumple, M.-G. Song, P. Pollet, Prof. C. A. Eckert, Prof. C. L. Liotta
School of Chemistry and Biochemistry
Georgia Institute of Technology
911 Atlantic Drive, Atlanta, GA 30332 (USA)
E-mail: charles.liotta@chemistry.gatech.edu

Supporting Information for this article is available on the WWW under http://dx.doi.org/10.1002/cssc.201300438.

Table 1. Silylamine structures, names, abbreviations, and gravimetric CO_2 uptake capacities after reaction with 1 bar CO_2 at 25 °C.

Silylamine	Abbreviation	CO_2 uptake $[mol_{CO_2}\, mol_{amine}^{-1}]$	$[mol_{CO_2}\, kg_{amine}^{-1}]$
variation of alkyl chain length between Si atom and amine			
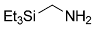 1-(aminomethyl)triethylsilane	TEtSMA	0.59 ± 0.01	4.09 ± 0.08
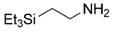 2-(aminoethyl)triethylsilane	TEtSEtA	0.59 ± 0.01	3.67 ± 0.03
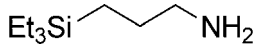 3-(aminopropyl)triethylsilane	TEtSA	0.63 ± 0.01	3.66 ± 0.04
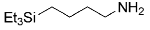 4-(aminobutyl)triethylsilane	TEtSBA	0.35 ± 0.03	1.9 ± 0.2
branching along the alkyl chain backbone			
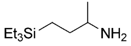 4-(triethylsilyl)butyl-2-amine	αMe-TEtSA	0.63 ± 0.03	3.36 ± 0.15
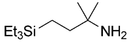 2-methyl-4-(triethylsilyl)butyl-2-amine	α,αDMe-TEtSA	0.48 ± 0.03	2.4 ± 0.2
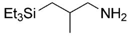 2-methyl-3-(triethylsilyl)propylamine	βMe-TEtSA	0.59 ± 0.01	3.15 ± 0.07
unsaturation in the alkyl chain backbone			
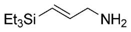 *trans*-3-(triethylsilyl)prop-2-en-1-amine	*trans*-TEtSA	0.61 ± 0.03	3.56 ± 0.20
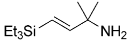 *trans*-2-methyl-4-(triethylsilyl)butyl-2-amine	*trans*-α,αDMe-TEtSA	0.47 ± 0.03	2.35 ± 0.16
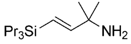 *trans*-2-methyl-4-(tripropylsilyl)butyl-2-amine	*trans*-α,αDMe-TPSA	0.40 ± 0.000	1.65 ± 0.000
secondary silylamines			
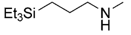 *N*-methyl-3-(triethylsilyl)propan-1-amine	STEtSA	0.65 ± 0.01	3.49 ± 0.05
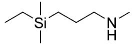 *N*-methyl-3-(aminopropyl)dimethylethylsilane	SDMESA	0.62 ± 0.02	3.87 ± 0.11
additional			
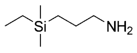 3-(aminopropyl)dimethylethylsilane	DMESA	0.42 ± 0.04	2.85 ± 0.24

how, despite having similar molecular weights, the properties of these 13 silylated amines differ substantially. The properties presented include CO_2-uptake capacity, reversal temperature, enthalpy of regeneration, and reversible ionic liquid viscosity.

Results and Discussion

Synthesis

The silylamines were prepared as follows. Detailed experimental procedures and characterization of the silylamines are included in the Supporting Information. Yields and synthesis procedures were not optimized as the goal was to evaluate the properties for CO_2 capture of the silylamines to establish structure–property relationships.

TEtSMA

TEtSMA was synthesized through a three-step procedure as highlighted in Scheme 2. The first step involved the Grignard reaction of trichloro(chloromethyl)silane with ethyl magnesium chloride to form triethylchloromethylsilane. The triethylsilyl phthalimidomethane intermediate was prepared by reaction of triethylchloromethylsilane with potassium phthalimide and subsequently reacted with hydrazine to afford TEtSMA in an overall 27 % isolated yield.

TEtSEtA

TEtSEtA was prepared as shown in Scheme 3. Triethylsilane was reacted with *N*-vinylphthalimide in the presence of platinum(0)-1,3-divinyl-1,1,3,3-tetramethyldisiloxane (Pt-DVDS) to yield phthalimide-protected 2-(aminoethyl)triethylsilane. The intermediate was then reacted with hydrazine to yield TEtSEtA in 25 % isolated yield.

TEtSA, DMESA, and TEtSBA

TEtSA and DMESA were prepared by the hydrosilylation of allyl amine and the corresponding silane (dimethylethylsilane or triethylsilylane, respectively) with Pt-DVDS in toluene at 110 °C to yield TEtSA (89 % isolated yield) and DMESA (58 % isolated yield) as shown in Scheme 4.

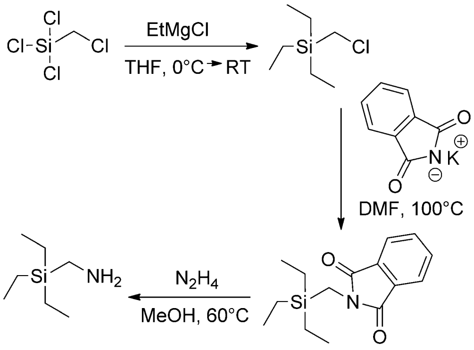

Scheme 2. Synthesis of TEtSMA.

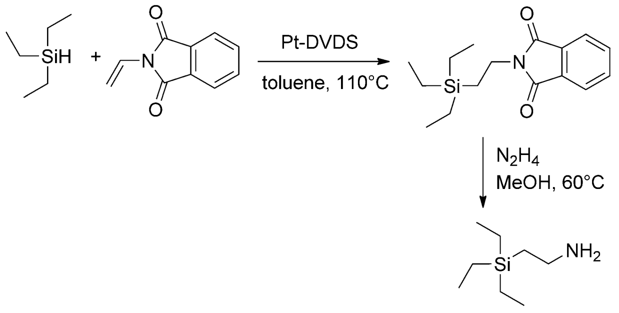

Scheme 3. Synthesis of TEtSEtA.

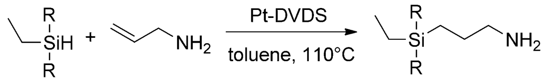

Scheme 4. Synthesis of TEtSA (R = CH_2CH_3) and DMESA (R = CH_3).

TEtSBA was formed by the hydrosilylation of 4-amino-1-butene with Pt-DVDS in toluene at 80 °C (Scheme 5; 66 % yield).

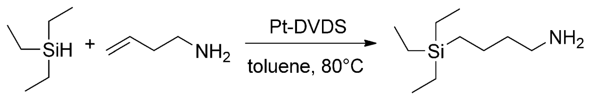

Scheme 5. Synthesis of TEtSBA.

αMe-TEtSA

The synthesis of αMe-TEtSA followed a Gabriel synthesis pathway from 3-chloro-1-butene (Scheme 6). 3-Chloro-1-butene was reacted with potassium phthalimide and K_2CO_3 in DMF. The resulting compound, 3-phthalimido-1-butene, was then reacted with Pt-DVDS and triethylsilane in toluene at reflux. Deprotection was achieved by using anhydrous hydrazine in anhydrous methanol at 60 °C to yield αMe-TEtSA in a 67 % isolated yield.

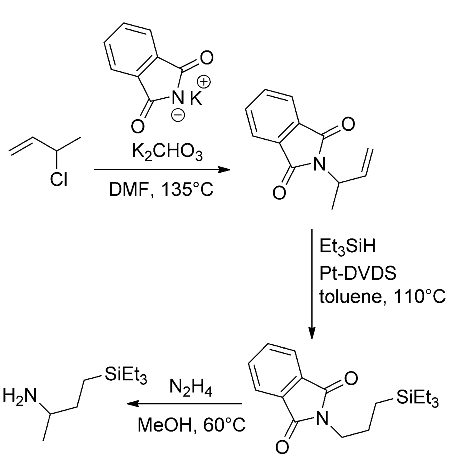

Scheme 6. Synthesis of αMe-TEtSA.

α,αDMe-TEtSA

Commercially available α,α-dimethylpropargylamine was reacted at room temperature with triethylsilane in the presence of Pt-DVDS and phosphatrane in THF (Scheme 7). The product, *trans*-2-methyl-4-(triethylsilyl)butyl-2-amine, was distilled after the evaporation of THF. The compound was then reduced under hydrogenation conditions in a Parr autoclave reactor with Pd on carbon in hexane at 50 °C to afford α,αDMe-TEtSA in an 80 % isolated yield.

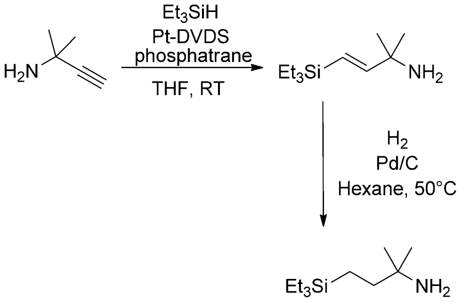

Scheme 7. Synthesis of α,αDMe-TEtSA.

βMe-TEtSA

The β-methyl derivative of TEtSA, βMe-TEtSA, was synthesized through the hydrosilylation of commercially available 2-methylallylamine (Scheme 8, 76 % isolated yield).

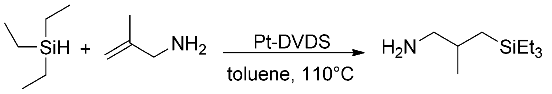

Scheme 8. Synthesis of βMe-TEtSA.

trans-*TEtSA,* trans-*α,αDMe-TEtSA, and* trans-*α,αDMe-TPSA*

The general reaction scheme for the synthesis of *trans*-TEtSA, *trans*-α,αDMe-TEtSA, and *trans*-α,αDMe-TPSA is shown in Scheme 9. For *trans*-TEtSA, propargylamine was reacted with triethylsilane at room temperature in the presence of Pt-DVDS in THF to provide the product in a 46 % isolated yield. For *trans*-α,αDMe-TEtSA and *trans*-α,αDMe-TPSA, α,α-dimethylpropargylamine was reacted at room temperature with the corresponding silane (triethylsilane or tripropylsilane, respectively) in the presence of Pt-DVDS and phosphatrane in THF to yield the desired silylamine. *trans*-α,αDMe-TEtSA and *trans*-α,αDMe-TPSA were obtained in 80 and 68 % isolated yield, respectively.

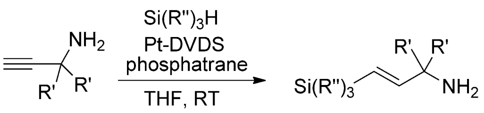

Scheme 9. Synthesis of *trans*-TEtSA (R′ = H; R″ = CH_2CH_3), *trans*-α,αDMe-TEtSA (R′ = CH_3; R″ = CH_2CH_3), and *trans*-α,αDMe-TPSA (R′ = CH_3; R″ = $CH_2CH_2CH_3$).

STEtSA and SDMESA

The synthetic strategy for the formation monomethylated TEtSA and DMESA is shown in Scheme 10. TEtSA or DMESA were reacted with ethyl formate under neat conditions in an Ar atmosphere at 60 °C. The amide was then reacted with $LiAlH_4$ in THF (1 м) in THF at 60 °C to yield STEtSA (73 % isolated yield) or SDMESA (49 % isolated yield).

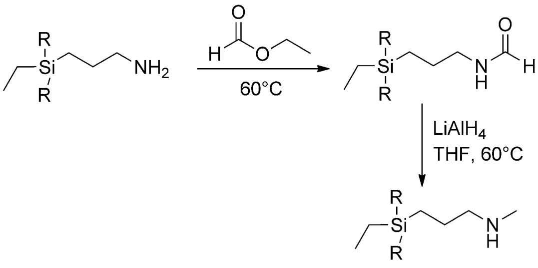

Scheme 10. Synthesis of STEtSA ($R=CH_2CH_3$) and SDMESA ($R=CH_3$).

CO_2 capacity

The equilibrium CO_2 uptake of each silylamine under 1 bar of CO_2 at 25 °C was measured by gravimetry (Table 1). The CO_2 uptake is reported both in moles of CO_2 per mole of amine as well as moles of CO_2 per kilogram of solvent. The former is useful to discern stoichiometric effects, whereas the latter is more useful to judge industrial viability compared to other solvent systems.

On average, the silylamines summarized in Table 1 exhibit an equilibrium CO_2 capacity of 0.59 moles of CO_2 per mole of amine. This combines CO_2 absorption from the chemical reaction of CO_2 with the silylamine and physical absorption of CO_2 into the newly formed ionic liquid. Previous silylamine studies have shown that under 1 bar of CO_2 at 25 °C, physical absorption contributes approximately 0.01–0.02 moles of CO_2 per mole of amine to the overall CO_2 capacity [0.59 moles of CO_2 per mole of 3-(aminopropyl)tripropylsilane) (TPSA)].[13] The majority of the CO_2 uptake is the result of the chemical reaction of CO_2 with the silylamine. The conventional stoichiometric CO_2 capacity of an amine that reacts with CO_2 to form ammonium-carbamate ion pairs is 0.5 moles of CO_2 per mole of amine. However, our silylamines exhibit an enhanced CO_2 capacity. An in-depth investigation of the chemical reaction of CO_2 with the silylamines has shown that a stabilized carbamic acid species is formed amidst a network of ammonium-carbamate ion pairs (Figure 1).[13] The results established that the theoretical CO_2 capacity for the chemical reaction was in fact 0.67 moles of CO_2 per mole of amine. Several of the silylamines (TEtSA, αMe-TEtSA, STEtSA, and SDMESA) discussed herein approach this limit (Table 1).

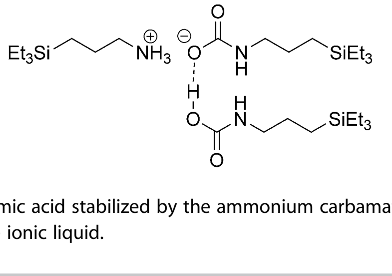

Figure 1. Carbamic acid stabilized by the ammonium carbamate ion of the TEtSA reversible ionic liquid.

Variation of the distance between the amine and the Si atom does not adversely affect the CO_2 capacity until the tether is increased to a butyl chain (Table 1). TEtSBA forms a low-melting solid immediately upon reaction with CO_2; the comparatively lower equilibrium CO_2 uptake (i.e., incomplete reaction) observed is likely the result of occlusion of the silylamine within the solid carbamate salt. Otherwise, the variation of the linker chain from methylene to ethylene and propylene did not alter the CO_2 uptake significantly; a deviation of only 0.02 moles of CO_2 per mole of amine is observed between TEtSMA, TEtSEtA, and TEtSA.

Compared to TEtSA, the inclusion of a single methyl group in the α position to the amine (αMe-TEtSA) does not affect the CO_2 capacity; both TEtSA and αMe-TEtSA show a CO_2 uptake of 0.63 moles of CO_2 per mole of amine. However, the introduction of a second methyl group at the α position (α,αDMe-TEtSA) decreases the CO_2 capacity on a molar basis by 27 %. The decreased CO_2 uptake is a result of the increased steric hindrance at the reactive amine site, which lowers the stability of the carbamate species formed upon reaction with CO_2. Interestingly, the inclusion of a methyl group in the β position relative to the amine (βMe-TEtSA) causes a slight decrease in the CO_2 capacity; βMe-TEtSA has a capacity of 0.59 moles of CO_2 per mole of amine compared to 0.63 moles of CO_2 per mole of amine for TEtSA.

Unsaturation along the alkyl chain backbone between the Si atom and amine has little effect on the CO_2 uptake compared to its saturated analogue. Unsaturated *trans*-TEtSA exhibits a CO_2 capacity of (0.61 ± 0.03) moles of CO_2 per mole of amine, whereas saturated TEtSA exhibits a similar CO_2 capacity of (0.63 ± 0.01) moles of CO_2 per mole of amine. Unsaturated *trans*-α,αDMe-TEtSA exhibits a CO_2 capacity of (0.47 ± 0.03) moles of CO_2 per mole of amine, whereas saturated α,αDMe-TEtSA shows a CO_2 capacity of (0.46 ± 0.01) moles of CO_2 per mole of amine. An additional unsaturated silylamine with a longer alkyl chain around the Si atom, *trans*-α,αDMe-TPSA, was also investigated and its CO_2 uptake was slightly lower than that of the other unsaturated silylamines at 0.40 moles of CO_2 per mole of amine.

The secondary silylamine STEtSA exhibits a CO_2-uptake capacity of (0.65 ± 0.01) moles of CO_2 per mole of amine, which is on a par with that of its primary amine analogue TEtSA ((0.63 ± 0.01) moles of CO_2 per mole of amine). The secondary silylamine SDMESA exhibits a significantly higher CO_2-uptake capacity (0.62 moles of CO_2 per mole of amine) than its primary amine counterpart, which reached a CO_2 uptake of only 0.42 moles of CO_2 per mole of amine. DMESA immediately forms a solid upon reaction with CO_2, whereas SDMESA does not.

The CO_2 uptake at 40 °C was investigated for a select group of silylamines to evaluate the effect of temperature on the CO_2 absorption (Table 2). An absorption temperature of 40 °C is representative of the flue-gas temperature of a post-combustion

Table 2. CO_2 uptake capacity at 40 °C for a select group of silylamines.

Silylamine	CO_2 uptake at 40 °C [$\text{mol}_{CO_2}\,\text{mol}_{\text{amine}}^{-1}$]	 [$\text{mol}_{CO_2}\,\text{kg}_{\text{amine}}^{-1}$]
TEtSA	0.603 ± 0.002	3.48 ± 0.01
α,αDMe-TetSA	0.46 ± 0.02	2.29 ± 0.08
βMe-TetSA	0.599 ± 0.003	3.19 ± 0.01

stream in a coal-fired power plant. Of the three silylamines investigated at 40 °C, only TEtSA showed a (modest) drop of 5 % in CO_2 capacity at this elevated temperature.

Reversal temperature

The reversal temperature is the point at which the reversible ionic liquid releases CO_2 and reverts back to the silylamine. We determined the reversal temperature of the reversible ionic liquids experimentally by using differential scanning calorimetry (DSC). The temperatures of the reversal events were determined by the intersection of the baseline of the event and the tangent to the peak of the event (see Supporting Information for an example thermogram).

The lower the temperature of reversal, the smaller the amount of energy required to heat the reversible ionic liquid from the capture temperature to the point at which the CO_2 is released. Of the structural modifications investigated, the effect of branching along the alkyl chain backbone, unsaturation of the propyl backbone, and the order of the amine (1° or 2°) showed the strongest influence on reversal temperature (Table 3). The reversal temperature of TEtSA is included as a baseline. These experimental results are in agreement with the trends predicted previously for the reversal temperatures of these ionic liquids by the quantum-chemical approach COSMO-RS.[12]

We examined the effect of the alkyl tether between the Si atom and the amine and found that decreasing the alkyl chain length from three C atoms (TEtSA) to two C atoms (TEtSEtA) results in the formation of a solid that melts at 49 °C. The reversal temperature increases by almost 40 °C. Unlike TEtSEtA, the additional reversible ionic liquids presented in Table 3 show a decrease in the reversal temperature from that of the TEtSA base comparison.

Table 3. Reversal temperature of reversible ionic liquids influenced by structural modifications.

Silylamine	Reversal temperature [°C]	Silylamine	Reversal temperature [°C]
TEtSMA	78 ± 5	TEtSEtA	109 ± 3[a]
TEtSA	71 ± 3	TEtSBA	84 ± 4[b]
αMe-TetSA	52 ± 2	α,αDMe-TEtSA	41 ± 6
βMe-TetSA	57 ± 7	*trans*-TEtSA	48 ± 2
trans-α,αDMe-TEtSA	11[c]	*trans*-α,αDMe-TPSA[d]	15 ± 2
STEtSA	30 ± 3	SDMESA	37 ± 2
DMESA	80 ± 8[e]		

[a] Formed solid (m.p. (49 ± 1) °C). [b] Formed solid [m.p. (66 ± 4) °C]. [c] Reversal temperature difficult to measure because of broad events in the DSC thermogram. [d] Bottom of reversal curve at 48 °C. [e] Formed solid [m.p. (66 ± 3) °C].

The introduction of a single methyl group, α (αMe-TEtSA) or β (βMe-TEtSA), to the amine results in a reduction of the reversal temperature of 19 and 14 °C, respectively. The introduction of two methyl groups α to the amine results in a further reduction in the reversal temperature as shown for α,αDMe-TEtSA (43 °C). As capture conditions dictate a flue-gas temperature of 40 °C, a reversal temperature at or below 40 °C would result in incomplete conversion to the reversible ionic liquid. Although the reversal temperature of α,αDMe-TEtSA is low, it evidences our ability to affect the reversible ionic liquid properties significantly by altering the silylamine structure.

The reversal temperatures of reversible ionic liquids with an unsaturated propyl chain (*trans*-TEtSA, *trans*-α,αDMe-TEtSA, *trans*-α,αDMe-TPSA) between the amine and Si atom were also investigated. A mixture of *cis* and *trans* unsaturated silylamines were initially proposed, however, only the *trans* isomers were synthesized. These unsaturated reversible ionic liquids show reversal temperatures that are over 20 °C less than those of their saturated counterparts. We postulate that this must be related to the entropic effect that results from the inflexible, locked conformation of the unsaturated reversible ionic liquids.

The reversal temperature of the secondary amines decreases significantly (30, 37 °C) compared to that of TEtSA (71 °C). Unlike the branched amines, both STEtSA and SDEMSA exhibit capacities equal to the corresponding primary amine at 25 °C. However, the capture conditions must be carefully balanced because these silylamines may not reach full conversion to the reversible ionic liquid at 40 °C.

Enthalpy of Regeneration

The enthalpy of regeneration is the primary contributor to the overall energy required to release absorbed CO_2 and regenerate the silylamine. The structural modifications presented here show both positive and negative deviations from the enthalpy of regeneration of the baseline silylamine TEtSA (Table 4).

The enthalpies of regeneration for the reversible ionic liquids were calculated from the DSC thermograms. Heat supplied to the system [$\text{kJ mol}_{CO_2}^{-1}$] was calculated based on the gravimetric uptake of CO_2.

An increase of the length of the alkyl tether between the amine and Si atom (TEtSBA) results in a significant increase in the heat of regeneration (152 $\text{kJ mol}_{CO_2}^{-1}$) with an enthalpy of regeneration almost double that of TEtSA (83 $\text{kJ mol}_{CO_2}^{-1}$). This may be a result of intramolecular interactions, which result in the stabilization of the ammonium-carbamate and carbamic acid species.[13]

As presented in the CO_2 capacity section, the introduction of two methyl groups in the α position to the amine (α,αDMe-TEtSA) results in the incomplete conversion of the silylamine to the reversible ionic liquid. This is likely because of steric hindrance, which causes destabilization of the carbamate ion.[14] As a result, the enthalpy of regeneration should be lower, although it appears to be higher than expected (114 $\text{kJ mol}_{CO_2}^{-1}$) compared to TEtSA. However, because of the decreased equilibrium CO_2 uptake of

Table 4. Enthalpy of regeneration of reversible ionic liquids influenced by structural modifications.[a]

Silylamine	Heat of regeneration $[\mathrm{kJ\,mol_{CO_2}}^{-1}]$	Silylamine	Heat of regeneration $[\mathrm{kJ\,mol_{CO_2}}^{-1}]$
TEtSMA	76 ± 7	TEtSEtA	91 ± 16[b]
TetSA	83 ± 6	TEtSBA	152 ± 19[c]
αMe-TEtSA	90 ± 5	α,αDMe-TEtSA	114 ± 16
βMe-TEtSA	89 ± 8	*trans*-TEtSA	85 ± 7
trans-α,αDMe-TetSA	7[d]	*trans*-α,αDMe-TPSA[e]	21 ± 6
STEtSA	77 ± 6	SDMESA	76 ± 2
DMESA	130 ± 14[f]		

[a] Heat of regeneration of reversible ionic liquids that formed solids includes both melting and CO_2-release DSC events. [b] Formed solid [m.p. (49 ± 1) °C]. [c] Formed solid [m.p. (66 ± 4) °C]. [d] Enthalpy difficult to measure because of broad events in the DSC thermogram. [e] Bottom of reversal curve at 48 °C. [f] Formed solid [m.p. (66 ± 3) °C].

α,αDMe-TEtSA, the enthalpy cannot be directly compared to that of its unbranched analogue (TEtSA); the enthalpies are calculated based on their respective equilibrium CO_2 uptake. The unsaturated amines, with branching in the α position to the amine (*trans*- α,αDMe-TEtSA, *trans*- α,αDMe-TPSA) show a decrease in the enthalpy of regeneration of 18 and 62 °C, respectively.

Reversible ionic liquid viscosity

The viscosities of the reversible ionic liquid species formed after reaction with 1 bar of CO_2 at 25 °C (at equilibrium conversions) are reported in Table 5. We recognize that some of the viscosities of the reversible ionic liquids reported at 25 °C are not industrially viable. Nevertheless, several important points must be emphasized: 1) viscosities at equilibrium conversion at 25 °C are important to characterize the structure–property relationships of the reversible ionic liquids, 2) industrial processes are usually conducted at temperatures higher than 25 °C (commonly 40 °C), which further reduces the viscosity of the reversible ionic liquid, and 3) in the real world it is not necessary for the CO_2 uptake to go to the full equilibrium CO_2 uptake, which allows an opportunity to control the viscosity of the system (see below).

The results given in Table 5 demonstrate that the manipulation of the silylamine structure can affect the reversible ionic liquid viscosity. The reversible ionic liquid viscosities reported here vary from < 100 to over 6000 cP at 25 °C.

The length of the alkyl tether between the amine and Si atom has a significant effect on the reversible ionic liquid viscosity. With only a methylene linker, the reversible ionic liquid viscosity is in the order of 2000 cP, whereas the reversible ionic liquid forms a solid with the longest linker (butylene). We anticipate that at intermediate lengths (ethylene and propylene) a trend of increasing reversible ionic liquid viscosity would be observed.

However, although TEtSA, which has a propylene linker, falls within the viscosity range of TEtSMA and TEtSBA, the reversible ionic liquid that has an ethylene linker, TEtSEtA, forms a solid after complete reaction with CO_2. It is not clear why TEtSEtA does not follow the viscosity trend of the other reversible ionic liquids. The trend exhibited by TEtSMA, TEtSA, and TEtSBA may be explained by the proximity to the Lewis acidic Si atom.

The branching along the alkyl chain backbone of the silylamine has a significant effect on viscosity. With an added methyl group in the α position to the amine (αMe-TEtSA), the reversible ionic liquid viscosity increases slightly (6915 vs. 6088 cP). However, when two methyl groups are in the α position (α,αDMe-TEtSA), the viscosity decreases to 1257 cP at 25 °C. The decrease in viscosity is likely because of the decreased CO_2 uptake. Unreacted silylamine (viscosity < 100 cP) could still be present. A 1000 cP decrease is seen in the reversible ionic liquid viscosity of βMe-TEtSA compared to that of TEtSA.

Table 5. Reversible ionic liquid viscosity of the silylamines after reaction with 1 bar CO_2 measured at 25 and 40 °C.

Silylamine	Viscosity [cP]	
	25 °C	40 °C
variation of the alkyl chain length between the Si atom and amine		
TEtSMA	2373 ± 206	625 ± 58
TEtSEtA	solid	solid
TEtSA	6088 ± 36	1303 ± 100
TEtSBA	solid	solid
branching along the alkyl chain backbone		
αMe-TEtSA	6915 ± 431	725 ± 164
α,αDMe-TEtSA	1257 ± 338	125 ± 22
βMe-TEtSA	5075 ± 141	1084 ± 62
unsaturation in the alkyl chain backbone		
trans-TEtSA	3889 ± 252	362 ± 19
trans-α,αDMe-TEtSA	< 100[a]	< 100[a]
trans-α,αDMe-TPSA	< 100[a]	< 100[a]
secondary silylamines		
STEtSA	135 ± 14	< 100[a]
SDMESA	117 ± 16	< 100[a]
additional		
DMESA	solid	solid

[a] Measurements below 100 cP are below the reliable detection limits of the instrument used.

Unsaturation in the alkyl chain backbone causes a 36 % decrease in the reversible ionic liquid viscosity at 25 °C for *trans*-TEtSA compared to the saturated reversible ionic liquid counterpart. A significant reversible ionic liquid viscosity decrease is also seen in *trans*-α,αDMe-TEtSA (< 100 cP) versus its saturated analogue α,αDMe-TEtSA (1257 ± 338 cP).[15] We found a similarly low reversible ionic liquid viscosity for *trans*-α,αDMe-TPSA. Notably, these two silylamines have a lower equilibrium CO_2 capacity than the other silylamines as they do not reach their full theoretical CO_2 capacity (0.67 moles of CO_2 per mole of amine) at 25 °C.

Although the secondary silylamine STEtSA does not exhibit a decreased CO_2 capacity relative to its TEtSA analogue, it has a markedly lower viscosity. At (135 ± 14) cP, the reversible ionic liquid viscosity of STEtSA is nearly 98 % lower than that of TEtSA. Similarly, although DMESA forms a solid upon reaction with CO_2, its secondary analogue, SDMESA has an ionic viscosity of only (117 ± 16) cP.

At 40 °C, the viscosity of the reversible ionic liquid drops by over 80 % on average (excluding those for which measurements are < 100 cP or form solids). For example, at 25 °C, the viscosity of TEtSMA is (2373 ± 206) cP, whereas the viscosity is only (625 ± 58) cP at 40 °C. As long as the reversal temperature is above 40 °C, a significant decrease in CO_2 capacity is not expected.

Control of the reversible ionic liquid viscosity

A unique feature of the reversible ionic liquid systems discussed herein is that the viscosity varies with CO_2 uptake following a hockey-stick-like relationship (Scheme 10). For 3-(aminopropyl)tripropylsilane (TPSA), the viscosity of the partially converted solvent (which contains both silylamine and reversible ionic liquid) is 620 cP at a CO_2 uptake of 0.45 moles of CO_2 per mole of amine at 25 °C.[11] However, with only a slight increase in CO_2 uptake to 0.50 moles of CO_2 per mole of amine, the viscosity increases by over 50 % to 1528 cP.

This curve is even more valuable for the results obtained at 40 °C (Figure 2). Compared to the 25 °C curve, it is immediately apparent that at 40 °C higher CO_2 uptakes can be achieved at lower viscosities. For example, at 25 °C with 0.45 moles of CO_2 per mole of amine, the viscosity of TPSA is 620 cP. If measured at 40 °C, a viscosity of 620 cP is not reached until an uptake that nears 0.52 moles of CO_2 per mole of amine. Notably, at a CO_2 uptake of 0.39 moles of CO_2 per mole of amine, the viscosity is only 144 cP—a viscosity that nears industrial viability.

A plot of CO_2 uptake versus viscosity for the branched amine α,αDMe-TEtSA at 25 °C is shown in Figure 3. Although α,αDMe-TEtSA does not reach the same CO_2 uptake as TPSA at 25 °C, the curves are similar in shape. The α branching affects only the end point; although the equilibrium CO_2 uptake is lower, the viscosity exhibits behavior similar to that of TPSA prior to the end point. At higher conversions, α,αDMe-TEtSA deviates slightly with a sharper rise in viscosity. For example, at 0.45 moles of CO_2 per mole of amine, the viscosity of α,αDMe-TEtSA is nearly 1500 cP, whereas TPSA does not reach a similar viscosity until 0.50 moles of CO_2 per mole of amine.

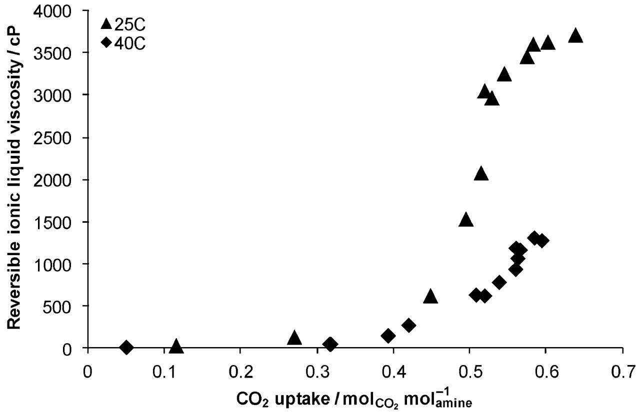

Figure 2. Viscosity versus CO_2 uptake for TPSA at 25 and 40 °C.

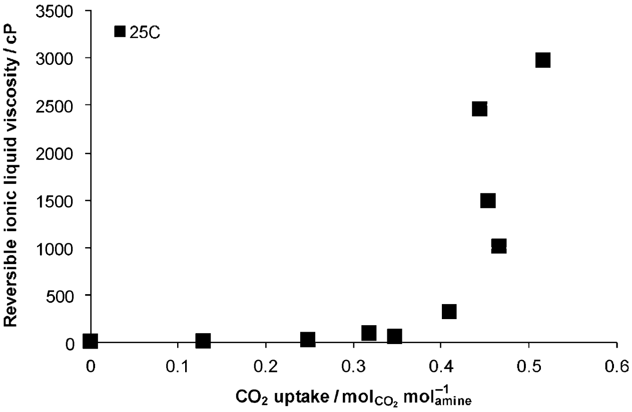

Figure 3. Viscosity versus CO_2 uptake for α,αDMe-TEtSA at 25 °C.

Conclusions

A systematic process to design CO_2-capture solvents that achieve a high CO_2 uptake—while minimizing viscosity and the energy required for reversal—has been presented. The influence of the length of the alkyl tether as well as the addition or change in the position of one or more methyl groups in the silylamine structure has a significant effect on the pertinent CO_2-capture properties of the reversible ionic liquids. 3-(Aminopropyl)triethylsilane (TEtSA) was used as a baseline silylamine to which structural modifications were made to establish structure–property relationships.

The CO_2 capacity was determined experimentally both in terms of moles of CO_2 per mole of silylamine as well as the more industrially relevant term of moles of CO_2 uptake per kilogram of silylamine. The influence of the length of the tether between the Si atom and the amine on CO_2 capacity is evident as silylamines with methylene and propylene tethers remain liquids in their ionic state and nearly achieve the maximum theoretical CO_2 uptake (0.67 moles of CO_2 per mole of amine), whereas the silylamine with a butylene linker immediately forms a solid upon reaction with CO_2. The energy required to regenerate the silylamine and release CO_2 is comparable for 1-(aminomethyl)triethylsilane (TEtSMA) and TEtSA, but the viscosity of TEtSMA is less than half of that of TEtSA. The length of the alkyl silylamine backbone has a definite influence on capacity, energy required for reversal, and viscosity.

The branching along the alkyl chain backbone was also investigated. The data show that the introduction of a methyl group in the α position to the amine (4-(triethylsilyl)butyl-2-amine; αMe-TEtSA) results in a reduction of 20 °C in the reversal temperature. Furthermore, the addition of a second methyl group in the α position to the amine (2-methyl-4-(triethylsilyl)-butyl-2-amine; α,αDMe-TEtSA) decreases the viscosity of the reversible ionic liquid to approximately a third of that of TEtSA, although the CO_2 uptake is affected. The effect of branching is further emphasized if the alkyl chain backbone is unsaturated. *trans*-2-Methyl-4-(triethylsilyl)butyl-2-amine (*trans*-α,αDMe-TEtSA) and *trans*-2-methyl-4-(tripropylsilyl)butyl-2-amine (*trans*-α,αDMe-TPSA) have viscosities of less than 100 cP in part because of reversal temperatures below 30 °C. The removal of the branching in the unsaturated backbone yields a reversible ionic liquid with a viscosity slightly higher than that of TEtSA but with a reversal temperature over 20 °C lower than that of the saturated species.

Table 6. Summary of the properties of TEtSMA and *trans*-TEtSA

Property	Unit	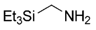 TEtSMA	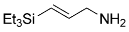 *trans*-TEtSA
CO_2 uptake at 25 °C	[mol_{CO_2} mol_{amine}^{-1}]	0.59 ± 0.01	0.61 ± 0.03
CO_2 uptake at 25 °C	[mol_{CO_2} kg_{amine}^{-1}]	4.09 ± 0.08	3.56 ± 0.20
reversal temperature	[°C]	78 ± 5	48 ± 2
enthalpy of regeneration	[kJ $mol_{CO_2}^{-1}$]	76 ± 7	85 ± 7
reversible ionic liquid viscosity at 25 °C	[cP]	2373 ± 206	3889 ± 252
reversible ionic liquid viscosity at 40 °C	[cP]	625 ± 58	362 ± 19

There is a strong effect of the order of the amine (1° and 2°) on the reversible ionic liquid properties as evidenced by the addition of a methyl group on the amine functionality (*N*-methyl-3-(aminopropyl)dimethylethylsilane, SDMESA). A 50-fold decrease in viscosity is observed for this reversible ionic liquid as well as a reversal temperature that is reduced below 40 °C compared to that of TEtSA.

Not only are we able to control the properties of the reversible ionic liquids by change of position or addition of methyl groups along the silylamine tether, but we can also control the viscosity by limiting the conversion to the reversible ionic liquid. The viscosity can be maintained below 300 cP while still able to achieve approximately 70 % conversion to the reversible ionic liquid at 40 °C. This behavior is not only unique to this system, but also serves as an additional parameter that may be used to meet criteria for industrial implementation.

Although the selection of a particular CO_2-capture solvent is dependent on the specifications of its end use application, we have identified two silylamine solvents for further investigation, TEtSMA and *trans*-3-(triethylsilyl)prop-2-en-1-amine (*trans*-TEtSA), the properties of which are summarized in Table 6. They both exhibit high CO_2-uptake capacities relative to the other silylamines studied, viable reversible temperatures, and reasonable enthalpies of regeneration. Their reversible ionic liquids have lower viscosities than most other silylamine reversible ionic liquids, and furthermore, by controlling the CO_2 uptake, the viscosity could be reduced to meet industry-operating specifications.

Experimental Section

Synthesis

The materials, experimental procedures, and the characterization for the synthesis of the silylamines are included in the Supporting Information.

Reversible Ionic Liquid Formation

For all of the reversible ionic liquids discussed, synthesis was performed as follows unless otherwise noted. A 2 dram vial was weighed; the silylamine (≈1 g) was added and the vial was weighed again. A porous fritted tube (Ace Glass, 10 mm gas dispersion tube, porosity C) was weighed and used to sparge dry carbon dioxide through the silylamine for 75 min at a flow rate of 200 mL min^{-1} at 25 °C and 1 bar. The resulting reversible ionic liquid, vial, and fritted tube were then weighed to determine the CO_2 uptake capacity at 25 °C. To determine the CO_2 uptake capacity at 40 °C, the same procedure was followed except that the vial and sample were placed in a 40 °C sand bath in thermal equilibrium with a heated gas line.

Instrumentation

Attenuated total reflectance (ATR) FTIR data were collected by using a Shimadzu IRPrestige21 spectrometer with a DLaTGS detector with 32 scans and a resolution of 1 cm^{-1} used in combination with a Specac, Ltd., heated Golden Gate ATR accessory with diamond crystal and zinc selenide lenses.[11,16]

^1H and ^{13}C NMR spectra were recorded by using a Varian Mercury Vx 400 instrument using $CDCl_3$ as the lock solvent. As a result of the high viscosities of the ionic forms, the reversible ionic liquids were synthesized in the NMR tube under solvent-free conditions, and a capillary tube that contained $CDCl_3$ was placed inside the sample.

The viscosities of all of the reversible ionic liquids were measured by using a Rheosys Merlin II viscometer with a temperature-controlled 2° cone and plate system. The densities of all of the silylamines and reversible ionic liquids (used in the gravimetric calculation of CO_2 uptake) were measured in triplicate by using an Anton Paar DMA 38 Laboratory Density Meter. Elemental analysis (C, N, H) of molecular liquids was performed at Atlantic Microlab in Norcross, GA. Samples were stored under inert gas and either delivered in person or sent by FedEx.

DSC measurements were used to determine the reversal temperatures of the reversible ionic liquids and the evaporation temperatures of the silylamines. The instrument used was a Q20 TA Instruments DSC; hermetically sealed aluminum pans were used, into which the compound under consideration (≈2 mg) was measured. The temperature was ramped from −40 to 400 °C at a rate of 5 °C min^{-1}, and the temperatures of the reversal or boiling events were determined by the intersect of the baseline of the event and the tangent to the peak of the event.

Acknowledgements

We thank Phillips 66 for their financial support of this research.

Keywords: amines · carbon · environmental chemistry · ionic liquids · structure–property relationships

[1] U.S. Energy Information Administration, Washington DC, **2011**.
[2] U.S. Energy Information Administration, Washington DC, **2000**.
[3] A. A. Olajire, *Energy* **2010**, *35*, 2610 – 2628.
[4] E. S. Rubin, H. Mantripragada, A. Marks, P. Versteeg, J. Kitchin, *Prog. Energy Combust. Sci.* **2012**, *38*, 630 – 671; A. B. Rao, E. S. Rubin, *Environ. Sci. Technol.* **2002**, *36*, 4467 – 4475.
[5] G. Sartori, D. W. Savage, *Ind. Eng. Chem. Fundam.* **1983**, *22*, 239 – 249.
[6] D. M. D'Alessandro, B. Smit, J. R. Long, *Angew. Chem.* **2010**, *122*, 6194 – 6219; *Angew. Chem. Int. Ed.* **2010**, *49*, 6058 – 6082.
[7] K. S. Fisher, K. Searcy, G. T. Rochelle, S. Ziaii, C. Shubert, Pittsburgh, PA, *Advanced Amine Solvent Formulations and Process Integration for Near-Term CO_2 Capture Success*, DOE Final Report (Grant DE-FG02-06ER84625), **2007**.
[8] P. G. Jessop, D. J. Heldebrant, X. W. Li, C. A. Eckert, C. L. Liotta, *Nature* **2005**, *436*, 1102 – 1102; L. Phan, D. Chiu, D. J. Heldebrant, H. Huttenhower, E. John, X. W. Li, P. Pollet, R. Y. Wang, C. A. Eckert, C. L. Liotta, P. G. Jessop, *Ind. Eng. Chem. Res.* **2008**, *47*, 539 – 545; L. Phan, J. R. Andreatta, L. K. Horvey, C. F. Edie, A.-L. Luco, A. Mirchandani, D. J. Darensbourg, P. G. Jessop, *J. Org. Chem.* **2008**, *73*, 127 – 132; B. E. Gurkan, J. C. de La Fuente, E. M. Mindrup, L. E. Ficke, B. F. Goodrich, E. A. Price, W. F. Schneider, J. F. Brennecke, *J. Am. Chem. Soc.* **2010**, *132*, 2116 – 2117.
[9] R. Hart, P. Pollet, D. J. Hahne, E. John, V. Llopis-Mestre, V. Blasucci, H. Huttenhower, W. Leitner, C. A. Eckert, C. L. Liotta, *Tetrahedron* **2010**, *66*, 1082 – 1090.
[10] V. Blasucci, C. Dilek, H. Huttenhower, E. John, V. Llopis-Mestre, P. Pollet, C. A. Eckert, C. L. Liotta, *Chem. Commun.* **2009**, 116 – 118; V. Blasucci, R. Hart, V. L. Mestre, D. J. Hahne, M. Burlager, H. Huttenhower, B. J. R. Thio, P. Pollet, C. L. Liotta, C. A. Eckert, *Fuel* **2010**, *89*, 1315 – 1319.
[11] A. L. Rohan, J. R. Switzer, K. M. Flack, R. J. Hart, S. Sivaswamy, E. J. Biddinger, M. Talreja, M. Verma, S. Faltermeier, P. T. Nielsen, P. Pollet, G. F. Schuette, C. A. Eckert, C. L. Liotta, *ChemSusChem* **2012**, *5*, 2181 – 2187.
[12] M. Gonzalez-Miquel, M. Talreja, A. L. Ethier, K. Flack, J. R. Switzer, E. J. Biddinger, P. Pollet, J. Palomar, F. Rodriguez, C. A. Eckert, C. L. Liotta, *Ind. Eng. Chem. Res.* **2012**, *51*, 16066 – 16073.
[13] J. R. Switzer, A. L. Ethier, K. M. Flack, E. J. Biddinger, L. Gelbaum, P. Pollet, C. A. Eckert, C. L. Liotta, *Ind. Eng. Chem. Res.* **2013**, *52*, 13159 – 13163.
[14] T. Mimura, H. Simayoshi, T. Suda, M. Iijima, S. Mituoka, *Energy Convers. Manage.* **1997**, *38*, S57 – S62.
[15] We could not accurately measure viscosities lower than 100 cP with our apparatus, but for the purpose of this paper it is sufficient to know they were below 100 cP (industrially viable limit).
[16] S. G. Kazarian, B. J. Briscoe, T. Welton, *Chem. Commun.* **2000**, 2047 – 2048.

Received: May 7, 2013